The Effect of Additives on Microcellular PVC Foams: Part II. Tensile Behaviour

Vipin Kumar, John E. Weller, Michelle Ma
and Romano Montecillo

Department of Mechanical Engineering,
University of Washington,
Seattle, WA 98195, USA

Robert R. Kwapisz

ALCOA Building Products,
Sidney, OH 45365, USA

SUMMARY

The effect of additives commonly used in PVC processing on the tensile behaviour of microcellular PVC was explored. Microcellular foams were produced from three different PVC formulations - one with a full range of additives, and two others with a minimum of additives. All formulations contained a basic level of internal lubricants required for extrusion. The results show no significant differences in the tensile properties between formulations. It is concluded that the presence of additives has no detrimental effect on the tensile behaviour of microcellular PVC foams.

INTRODUCTION

The field of microcellular plastics has seen consistent growth since its inception[1-5], with a wide variety of thermoplastics being successfully foamed. Microcellular PVC foams with a wide range of densities have been produced using carbon dioxide[6,7]. Due to the large volume of PVC used in building and construction industries, a considerable potential exists for application of microcellular PVC leading to associated savings in materials and transport costs. A key question to be answered before industrial applications can be developed is: what is the effect of the large amount of additives and other processing aids used in PVC processing on the structure and mechanical behaviour of microcellular PVC foams? In Part 1 of this investigation[8], it was found that commonly used additives do not adversely affect foam growth dynamics, even though these additives lead to microstructures that are markedly different than those seen previously. In this paper the effects of additives and microstructure on the tensile behaviour of microcellular PVC foams are explored.

Solid-state microcellular foams are polymeric foams where the average size of the cells is of the order of 10 μm. Such small cells can be produced when there is limited bubble growth and extremely high cell nucleation. In addition to very small cell size and extremely high cell nucleation density, microcellular foams are also characterised by their inherently layered structure: they are always produced with a very homogeneous foamed core surrounded by an integral unfoamed skin. This skin provides the foam with the look and feel of a solid material.

Microcellular foams are produced in a two-stage batch process. In the first stage of the process, an inert gas is introduced to a polymer sample through diffusion - traditionally, nitrogen and carbon dioxide have been used due to their high solubility in many thermoplastics. The polymer samples are placed in a pressure vessel where the gas is introduced at a relatively high pressure. Over time, the polymer absorbs the gas, and eventually becomes saturated. Saturation occurs when the sample does not absorb any more gas and the concentration of gas is uniform throughout the sample. The time required to saturate a sample may range from several hours to several weeks, depending on the polymer-gas system and the thickness of the sample.

In the second stage of the process, the sample is removed from the pressure vessel and heated, causing an extremely large number of bubbles to nucleate and grow. Typically, a saturated sample is foamed by placing it in a heated bath of glycerine or water at a temperature near the glass transition temperature of the virgin polymer. When the temperature of the sample is high enough, a very large quantity of cells nucleate over a short period of time and begin to grow. The final size of the cells depends on the length of time the polymer is immersed in the bath and the temperature of the bath. These process variables are referred to as the foaming time and foaming temperature respectively.

Microcellular PVC was first produced by Kumar and Weller[6], who showed that a wide range of microstructures can be produced in the PVC-CO_2 system and that foams with densities ranging from 10% of the solid PVC and higher could be produced. They investigated the effects of foaming temperature and foaming time on various foam characteristics and found that nucleation densities typically range from 10^7 to 10^{11} cells per cubic centimetre of PVC. Holl et al.[8] evaluated the effects of various additives (processing aids, stabilizers, stearate, etc.) on the microstructures of microcellular PVC. They found that additives can significantly alter the foam microstructure, changing not only the cell nucleation density, but the type and distribution of bubbles produced. This study reports the effect of additives on the tensile properties of microcellular PVC.

EXPERIMENTAL

Three PVC formulations were tested in this study, denoted PVC-A, PVC-B and PVC-C respectively. The compositions of the formulations are given in Table 1. PVC-A is a formulation used in a vinyl siding type of product. The PVC-B and PVC-C formulations differ from PVC-A in that the majority of the additives have been removed; only those additives required to successfully extrude the material were included. The PVC-B and PVC-C formulations only differ in the amount of Stearate added. These three formulations were extruded into approximately 1.0 mm thick sheets using a twin screw extruder with a 15.2 cm (6 inch) die. The specimens were then cut into rectangles approximately 5 cm by 15 cm. Half of these specimens were cut with the longer dimension in the extrusion direction, and the other half were cut with the longer dimension orthogonal to the extrusion direction. For each formulation and orientation, 35 specimens were produced. Five of these 35 specimens were left unprocessed, and the remaining were foamed. The densities of the PVC formulations were 1410, 1390 and 1380 kg m^{-3} for PVC-A, PVC-B and PVC-C respectively.

The specimens were saturated in a pressure vessel for 120 hours using CO_2 at 6 MPa and 40°C. After saturation, they were removed from the pressure vessel, allowed to desorb gas for 4 minutes, and then were foamed in a glycerine bath at various foaming temperatures for 240 seconds. These different foaming temperatures produced foams of different relative densities (density of the foam divided by the density of the solid, unfoamed material) ranging from 0.38 to 1.0. The foaming

Table 1 PVC formulations

	PVC-A[1] (phr) [3]	PVC-B[2] (phr)	PVC-C[2] (phr)
PVC	100	100	100
Stabiliser	0.8	1.5	1.5
Wax	1.0	1.0	1.0
Stearate	1.25	0.5	1.0
Calcium carbonate	10	0	0
Other[4]	6.4	0	0

1. PVC-A is a standard commercial formulation
2. PVC-B and PVC-C formulations are additive-free except for the essential stabiliser system and external lubricant (to allow satisfactory extrusion processing without excessive degradation)
3. phr designates parts per hundred by weight relative to the PVC in the blend
4. Other additives include processing aids, impact modifiers, etc.

conditions used in this study are shown in Table 2. After foaming, the samples were quenched in 20°C water and were left at atmospheric conditions for 70 days to allow the remaining CO_2 to escape. The specimens were then cut into the shape of an ASTM-D638 type IV tensile specimen using a die. The tensile specimens were tested according to ASTM-D638 specifications at a crosshead rate of 10 mm min^{-1}. A 25.4 mm (1.0 inch) extensometer was attached to the gauge section of all specimens during the initial portion of the tests. After the extensometer was removed, displacement was approximated from the crosshead displacement. Five specimens were tested at every condition.

Table 2 Foaming conditions used to produce the specimens in this study

Saturation pressure (MPa)	Saturation temp. (°C)	Saturation Time (hours)	Desorbtion time (min)	Foaming temp. (°C)	Foaming time (sec)	Approximate relative density*
6	40	120	4	51.4	240	0.93
6	40	120	4	58.3	240	0.88
6	40	120	4	65.9	240	0.72
6	40	120	4	73.8	240	0.56
6	40	120	4	81.8	240	0.38
6	40	120	4	89.9	240	0.40

*The foam relative density varied slightly depending on PVC formulation

RESULTS AND DISCUSSION

Table 3 gives the tensile properties of the three PVC formulations in both the extrusion and the orthogonal direction. It may be seen that the extrusion direction properties are generally superior to the orthogonal direction properties due to the alignment of the polymer chains imparted by the extrusion process. For example, for PVC-A the ultimate tensile stress (tensile strength) in the extrusion direction was 60.5 MPa, while in the orthogonal direction the tensile strength was 38.3 MPa. The orthogonal direction properties for PVC-C show relatively large reductions and variations. It was noted that tensile strength, strain at break, and toughness values for orthogonal direction of PVC-C specimens were the lowest of all tests conducted. Since this study focused on the effect of additives, and not on the effect of molecular alignment produced in extrusion, no effort was made to quantify this further. The main thrust of this paper will primarily discuss the results of tensile tests conducted on

Table 3 Tensile properties of unfoamed PVC formulations (values in parentheses are the standard deviation)

PVC formulation	Test direction	Tensile modulus (MPa)	1% offset yield stress (MPa)	Ultimate tensile stress (MPa)	Strain at break (mm mm^{-1})	Toughness (J cm^{-3})
PVC-A	extrusion	2732 (157)	46.0 (3.2)	60.5 (2.6)	3.11 (0.13)	106.4 (5.9)
	orthogonal	2378 (91)	41.0 (0.3)	38.3 (2.5)	3.2 (0.75)	112.1 (28.5)
PVC-B	extrusion	2967 (90)	52.6 (0.9)	58.0 (3.3)	2.01 (0.19)	99.1 (12.3)
	orthogonal	2750 (28)	49.9 (0.3)	40.6 (5.4)	2.31 (1.47)	88.8 (60.1)
PVC-C	extrusion	2960 (64)	53.5 (3.9)	56.8 (5.5)	1.78 (0.34)	86.4 (20.7)
	orthogonal	2623 (100)	47.7 (0.8)	35.0 (2.6)	0.76 (0.60)	27.5 (22.9)

PVC-A. PVC-B and PVC-C in the extrusion direction only. These data are represented by solid circles, squares, and triangles, respectively in all the figures.

Figure 1 shows typical stress-strain curves for the PVC-A formulation at different relative densities. Several significant observations can be made about the tensile behaviour of microcellular PVC directly from this figure. First, as the relative density decreased, the overall engineering stress at a particular strain also decreased. This translated into a lower

yield stress, lower ultimate tensile strength, and lower toughness relative to solid PVC. Surprisingly, the strain at break appears to change relatively little with changes in foam density, and varies from 1.7 to 2.1 mm mm^{-1} for all results shown in Figure 1. Secondly, there is a distinct change in shape of the stress-strain curve in the vicinity of the yield point. For the unprocessed PVC-A and the higher relative density foams, there is a distinct stress maximum that provides a well defined yield stress. In the lower relative density foams however, this stress maximum disappears. For the microcellular PVC-A formulation the maximum disappeared at a relative density of approximately 0.55, similar to the behaviour observed in microcellular polycarbonate[10]. Since there is no distinct stress maximum for the lower relative density foams, the traditional definition of the yield point cannot be used. In this paper the yield stress is based upon an offset method as follows. For the unprocessed PVC-A shown in Figure 1, the traditional definition of the yield point would be at the location of the local stress maximum. Alternatively, the yield point can be defined by the intersection of the stress-strain curve with a line whose slope is equal to the initial slope of the stress-strain curve that has been offset by a strain of one percent. This method of defining the yield point is similar to the widely used 0.2% offset method used for metals.

Figure 1 Typical engineering stress-strain curves for microcellular PVC at various relative densities. (PVC-A formulation in the extrusion direction)

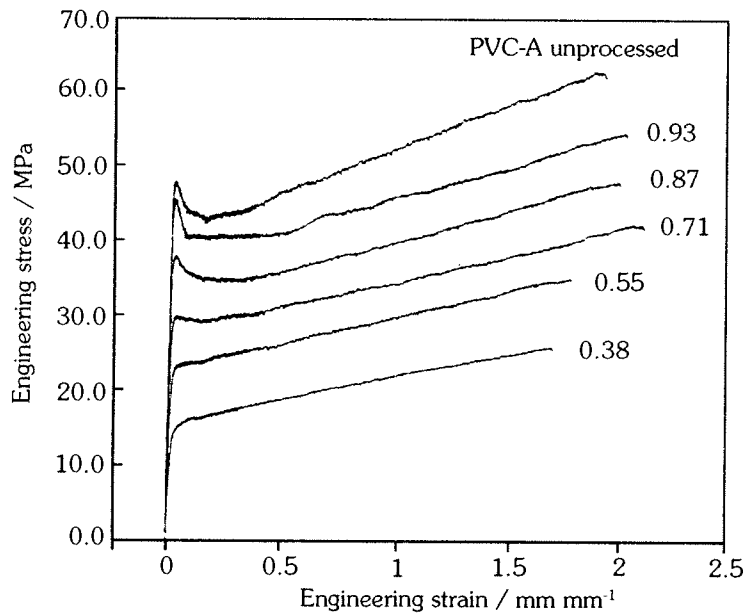

Figures 2 and 3 show plots of the tensile modulus and yield stress respectively, as a function of the foam relative density. The data at the relative density of 1.0 corresponds to the solid (unfoamed) PVC, and is presented here for comparison to foam properties. It was found that the

Figure 2 Tensile modulus as a function of relative density

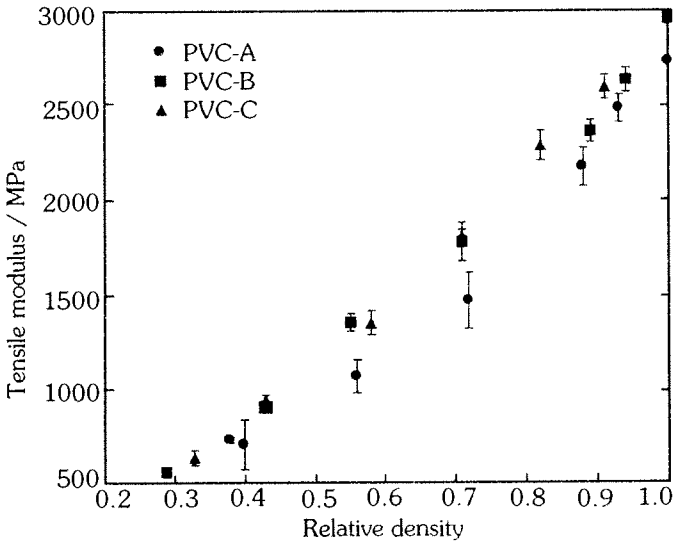

Figure 3 Yield stress as a function of relative density

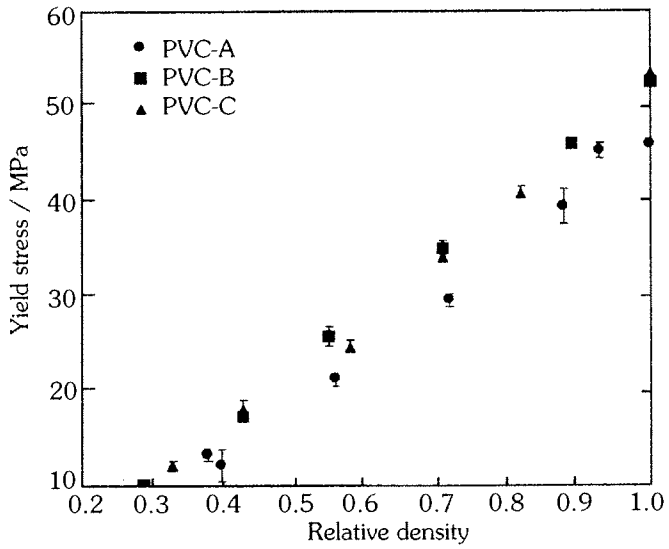

trends for PVC-A, the formulation with additives, were barely distinguishable from the data for PVC-B and PVC-C in both of these figures when the relative density was below 0.5. This indicates that the additives present in PVC-A do not have any significant effect on the modulus and yield strength of microcellular PVC foams of low relative density. However, in the range of relative density from 0.5 to 1.0 formulation PVC-A showed a significant but small reduction in both tensile modulus and yield stress compared with PVC-B and PVC-C. It was generally thought that this was attributable to the relatively high concentration of $CaCO_3$ in PVC-A which is generally accepted as a non-reinforcing filler in PVC formulations. At relative densities above 0.5, it was therefore postulated that the filler somewhat compromised the mechanical properties. Conversely, the increase in void fraction at relative densities below 0.5, provided a significant enough strength reduction in the system to mask the effect of $CaCO_3$ inclusion.

This effect was not observed in ultimate properties where the data in Figure 4 is compared to assess the effect of the presence of additives on the tensile strength of foams. Again it was found that there was no significant difference, at a given foam density, between the strength of PVC-A foams compared to those from formulations PVC-B and PVC-C. Thus, the difference in microstructure reported in Part 1 of this investigation, namely the polydisperse microstructure observed in PVC-A, compared to

Figure 4 Tensile strength as a function of relative density

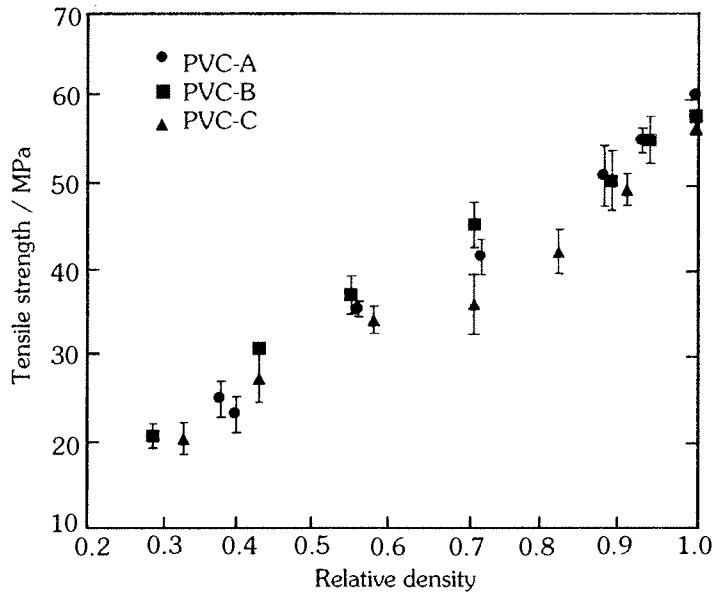

monodispersed structures for PVC-B and PVC-C, appear to have no significant effect on the tensile strength of the microcellular PVC foams. It was also noted that the overall trend exhibited by the tensile strength as a function of foam relative density is consistent with that reported by Matuana et al[7].

The toughness is plotted in Figure 5 as a function of the relative density. The toughness, which is defined as the area under the stress-strain curve, is the energy per unit volume required to fracture a material. From Figure 1 it is apparent that the area under the stress-strain curve becomes smaller as the foam density decreases. This is shown quantitatively in Figure 5, where the toughness ranges from approximately 100 J cm^{-3} for solid PVC at a relative density of 1.0 to 20 J cm^{-3} at a relative density of 0.3. Figure 5 also shows that the toughness of PVC-A is equal to or higher than the toughness of PVC-B and PVC-C. Thus the presence of additives does not necessarily have a detrimental effect on the toughness of microcellular PVC foams. Indeed, impact modifiers are often present in standard formulations to maintain and improve fracture toughness.

Figure 5 Toughness as a function of relative density

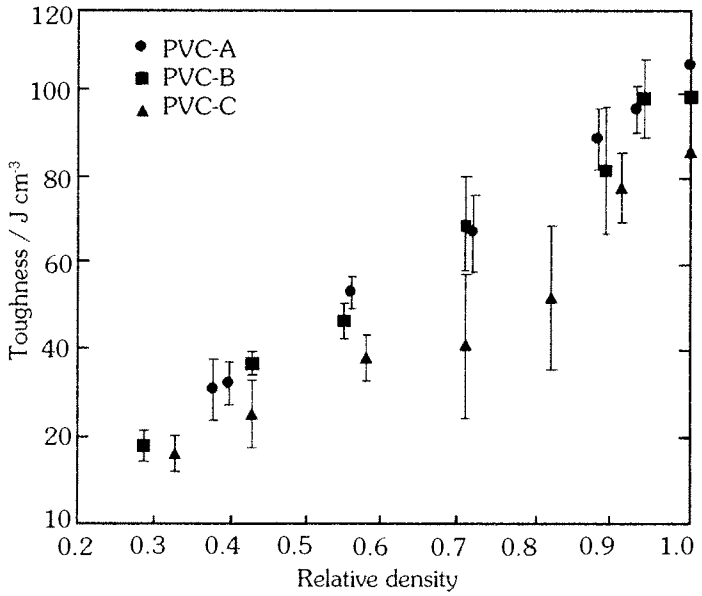

It is customary to represent the mechanical properties of foams on a relative basis. In Figures 6 and 7 the relative tensile modulus and relative tensile strength, respectively, have been plotted as a function of the foam relative density for all PVC formulations and for both the extrusion and

Figure 6 Relative tensile modulus as a function of relative density

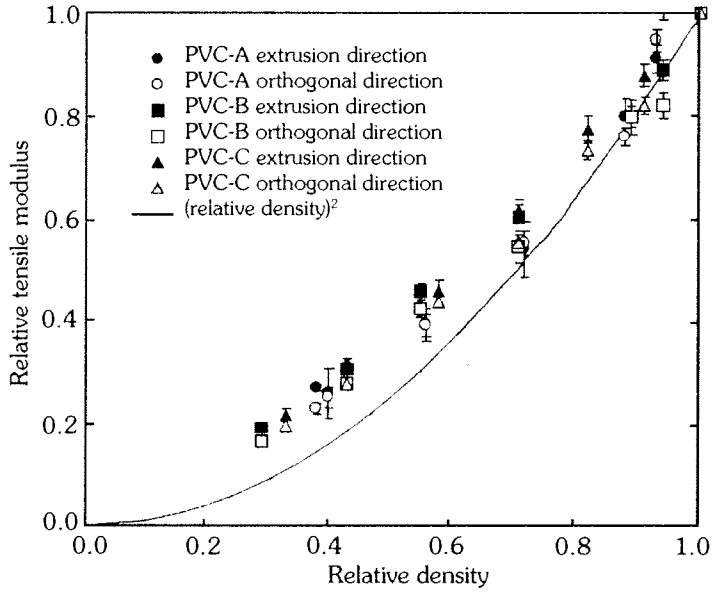

orthogonal directions. The relative property, for example the relative tensile strength, is obtained by dividing the tensile strength of the foam by the tensile strength of the corresponding solid PVC specimen. It may be seen from Figure 6 that all of the tensile modulus data lies close together. Thus stiffness of microcellular PVC foams is not significantly affected by differences in PVC formulations or directionality relative to the extrusion direction. It can also be seen that the relative modulus is well reasonably described by the square of the relative density. This behaviour is consistent with other microcellular foams[10] as well as cellular materials in general[11].

Figure 7 shows a plot of the relative tensile strength as a function of the relative density. The rule of mixtures model[11] suggests that the tensile strength should be proportional to the fraction of solid polymer in the foam. This relationship for the strength of foams represents an upper bound and assumes that the processing steps to produce the foam have not changed the properties or influenced the behaviour of the solid polymer. Figure 7 shows that the solid data symbols corresponding to the extrusion direction for the three PVC formulations, is generally well described by the rule of mixtures prediction. However, much of the data for the orthogonal direction tests (the open symbols) lies above the rule-of-mixtures line. This behaviour is due to the significantly lower tensile strength of the solid PVC in the orthogonal direction (see Table 3), giving

Figure 7 Relative tensile strength as a function of relative density

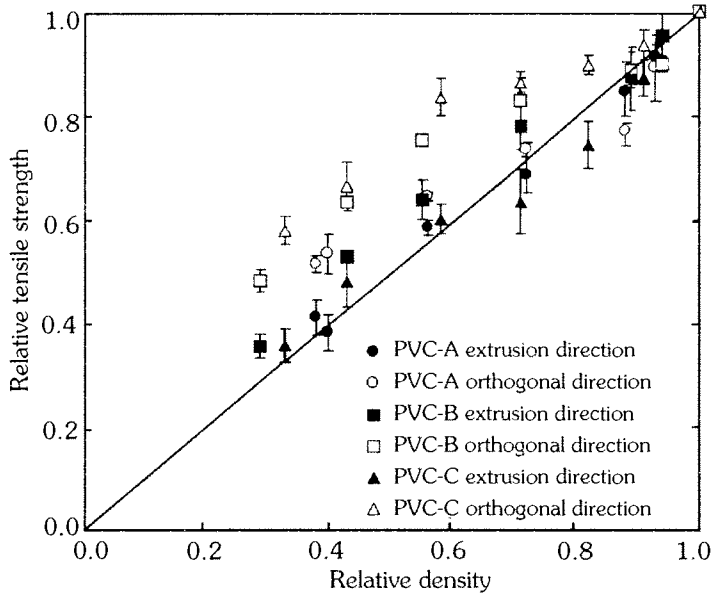

rise to a higher relative tensile strength. The actual tensile strength of the foam at a given relative density in the orthogonal direction is lower than that for the extrusion direction. Thus the relative property data can sometimes be misleading, as in the present case, and the reader is advised to exercise caution when comparing data presented on a relative basis.

CONCLUSIONS

The key conclusions from this study can be stated as follows:

1. There is no significant difference between the tensile properties of PVC-A, with 16.5% additives, as compared to PVC-B and PVC-C which formulated for minimum additive concentration. Thus the markedly different microstructures for these formulations observed in Part 1 of this study do not result in significantly different tensile properties such as tensile strength, tensile modulus, and toughness.

   This conclusion is significant since it shows that relatively large amounts of additives used in processing PVC do not necessarily deteriorate the mechanical properties of microcellular PVC foams. Thus the microcellular process can be applied to commonly used PVC formulations in order to develop novel materials for various commercial applications.

2. The data for PVC-A is especially significant as it represents tensile behaviour of microcellular PVC foams that may be typically used in practice. The tensile properties in extrusion direction are in general superior to properties in the orthogonal direction.
3. The tensile behaviour of microcellular PVC foams is consistent with other systems such as microcellular polycarbonate.
4. It is concluded that relative property data can sometimes give rise to misleading comparisons.

ACKNOWLEDGEMENTS

This research was supported by the UW-Industry Cellular Composites Consortium. This support is greatly acknowledged. The authors would also like to thank ALCOA Building Products for providing the materials used in this study.

REFERENCES

1. Martini J.E., Suh N.P. and Waldman F.A., SPE Tech. Papers, **28**, (1982), 674
2. Kumar V. and Suh N.P., Poly. Eng. Sci., **30**, (1990), 1323
3. Park C.B. and Suh N.P., Poly. Eng. Sci., **36**, (1996), 34
4. Ramesh N.S., Rasmussen D.H. and Campbell G.A., Poly. Eng. Sci., **31**, (1991), 1657
5. Kumar V. and Schirmer H.G., SPE Tech. Papers, **41**, (1995), 2189
6. Kumar V. and Weller J.E., Int. Poly. Proc., **8**, (1993), 73
7. Matuana-Malanda L., Park C.B. and Balatinecz J.J., Cell. Polym., **17**, (1998), 1
8. Holl M.R., Ma M. and Kumar V., Cell. Poly., **17**, 4, (1998), p. 271
9. Kumar V. and Weller J.E., ASME J. Eng. Ind., **116**, (1994), 413
10. Weller J.E., The Effects of Processing and Microstructure on the Tensile Behaviour of Microcellular Foams, PhD dissertation, University of Washington, Seattle, WA, (1996)
11. Gibson L.J. and Ashby M.F., Cellular Solids, Structure and Properties, Pergamon Press, New York, (1998)

Impact Strength of High Relative Density Solid State Carbon Dioxide Blown Crystallizable Poly(Ethylene Terephthalate) Microcellular Foams

Vipin Kumar[a,c], Richard P Juntunen[a], and Chris Barlow[b]

University of Washington,
Seattle, Washington 98195, USA

SUMMARY

In this paper, processing conditions for producing high relative density microcellular CPET foams using CO_2 as a blowing agent are described. Starting with solid CPET, foams with relative densities between 0.5 to 1.0 were produced. Results of instrumented impact tests conducted at various temperatures ranging from room temperature to -40°C are presented. The CPET foams exhibit excellent impact properties in the range of temperatures explored.

INTRODUCTION

The solid-state batch process has previously been applied to crystallized poly(ethylene terephthalate) CPET to produce a family of microcellular foams[1]. An interesting phenomenon observed during the process characterization is the additional crystallization of CPET at room temperature in the presence of sufficiently high gas concentrations. This onset of crystallization during the gas uptake stage of the solid-state batch foaming process at sufficiently high CO_2 pressures has also been observed in poly(ethylene terephthalate) PET[1-5] but not in PETG[6]. An immediate effect of the crystallization is an increased glass transition temperature (T_g), thus requiring higher foaming temperatures. Baldwin and Suh[1] observed that crystalline foams possessed smaller cell nucleation density compared to amorphous foams, accompanied by smaller cells. The mechanisms for these observations proposed by Baldwin and Suh[1], are: 1) the crystals act as heterogeneous cell nucleation sites, providing larger,

[a] Department of Mechanical Engineering, Box 352600
[b] Department of Materials Science and Engineering, Box 352120
[c] Author to whom correspondence should be addressed

Footnote: Based on a paper first presented at the Society of Plastics Engineers "Foams 99" Conference, Parsipanny, New Jersey, USA, October 1999

stable nuclei and 2) the crystals act to stiffen the polymer matrix, thereby preventing the cells from growing large enough to coalesce. This crystallization is thus desirable for the microcellular process.

Figure 1 shows a schematic of the solid-state batch process in which the polymer is first saturated with a gas, and then heated to a temperature above the glass transition temperature of the polymer-gas system, which can be significantly below the T_g of the virgin polymer due to the plasticizing effect of the gas. This batch process has been converted to a semi-continuous process, shown schematically in Figure 2, that allows essentially continuous production of microcellular foam sheets[7,8]. The words 'solid-state' underscore the fact that the polymer remains in the solid state during the entire process, which enhances the properties of the resulting foams.

This study undertakes to determine the impact behaviour of high relative density CPET foams. Both Gardner impact tests and instrumented impact tests were conducted. These impact tests were performed at varying temperatures between 22.2°C (72°F) and -40°C (-40°F).

Figure 1 Solid-state batch foaming process schematic

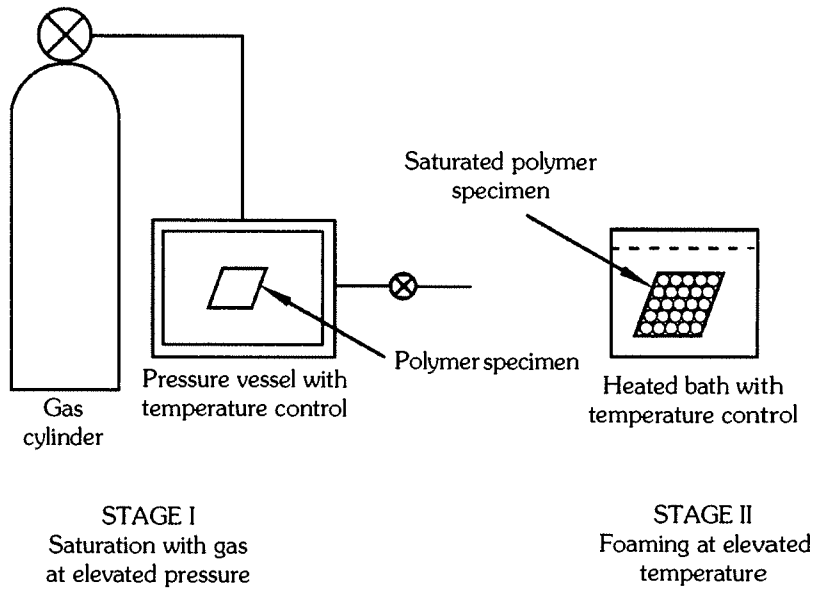

Figure 2 Semi-continuous foaming process schematic

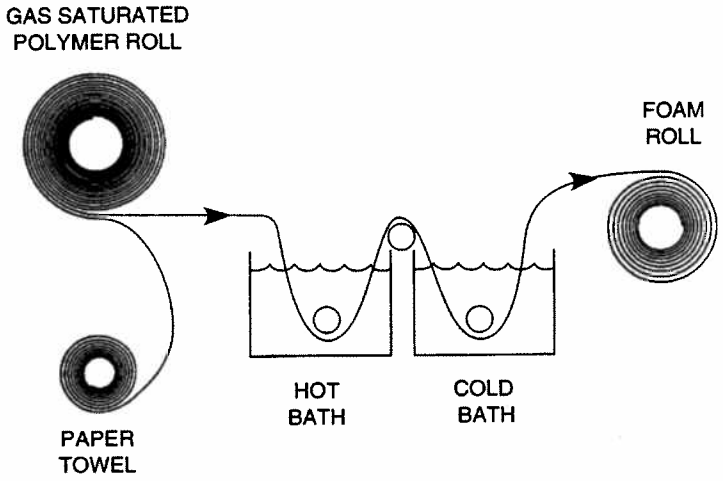

EXPERIMENTAL

Material

Eastman Kodak's Eastapak™ CPET 12822 sheet 0.7 mm (0.028 in.) thick, with 8% impact modifier and 3% nucleating agent, was used in this study. The impact modifier is a cross-linked acrylic impact modifier (rubber) with a particle size less than 1 μm and the nucleating agent used is a LLDPE based nucleating agent containing some stabilizers. A small amount of inorganic nucleant is also added. The density of this composition was determined to be 1.30 g/cm^3 using ASTM D792-91 "Standard Test Methods for Density and Specific Gravity of Plastics by Displacement". The T_g and weight percent crystallinity (W_c) were determined to be 75°C and 10.4, respectively, using differential scanning calorimetry (DSC).

Solubility Measurements

Samples measuring approximately 25 mm x 25 mm were cut from the CPET sheet. Gas uptake curves were produced by taking the initial mass of the sample, and checking the gas uptake periodically by removing the sample from the pressure vessel and taking a mass measurement. Samples were measured on a Mettler AE 240 precision balance, with an accuracy of 10 μg. Three saturation pressures (3, 4 and 5 MPa) were chosen to monitor the CO_2 solubility and to demonstrate the crystallization

of the CPET at increased saturation pressures. The CO_2 pressure or saturation pressure (P_{SAT}) and saturation temperature (T_{SAT}) were regulated to ±0.1 MPa and ±1°C respectively. The saturation temperature for all experiments was 25°C (77°F).

Specimen Saturation

Strips of material measuring approximately 5 m x 6.5 cm were cut from the CPET sheet. Seven strips were prepared to cover the testing conditions anticipated. These pieces of material were then paired with porous pieces of paper of the same size and wound into a roll. The rolls were then placed into a pressure vessel and pressurized with CO_2. The CO_2 pressure or saturation pressure (P_{SAT}) and saturation temperature (T_{SAT}) were regulated to ±0.1 MPa and ±1°C respectively. The vessels were then maintained at 5 MPa (725 psi) and 25°C (77°F). The results from the solubility measurements were used to determine the time needed to achieve maximum CO_2 concentration.

Specimen Foaming

After the samples were saturated, they were removed from the pressure vessel and processed using the semi-continuous process[7,8]. To produce a sheet of foam, for example, a sheet of CPET was placed on a sheet of gas permeable material and the two layers of material were rolled to form a roll consisting of layers of polymer interweaved with gas permeable material. The roll was then passed through a hot bath and foamed at temperatures ranging from 50°C (122°F) to 90°C (194°F). All foaming was conducted at atmospheric pressure. It was found that a cold bath was not needed, as the foams cooled sufficiently quickly under ambient conditions.

Falling Weight Impact Tests (Gardner Impact)

Foams from the above foaming experiments were selected for impact testing based on their microstructure and feasibility in producing flat specimens. Twenty six specimens, measuring 50mm x 50mm were then cut from the corresponding processed sheet to assemble a sample set to be impact tested. The foams were then tested on a BYK Gardner Impact Tester with a falling weight capacity of 36.2 Joules (26.7 ft-lbs.). About 6 foamed specimens were needed to approximately determine the mean-failure height. Twenty additional samples were then tested to produce a statistically precise measurement of the impact strength. ASTM D5420-

93 "Standard Test Method for Impact Resistance of Flat, Rigid Plastic Specimen by Means of a Striker Impacted by a Falling Weight (Gardner Impact)" was followed, employing tup geometry GE (striker diameter: 12.70 ± 0.10 mm, support plate inside diameter: 16.26 ± 0.025 mm). Immediately before impact testing, 10 samples from each sample set were measured for thickness, weighed for concentration of gas still in the matrix, and their densities were calculated using ASTM D792-91. From these measurements an average thickness, average gas concentration, and average density for each sample set was determined. A relative density for each sample set was then calculated from the foam average density and the density of the parent material. All impact tests were conducted at room temperature and atmospheric pressure.

Instrumented Impact Tests

Circular samples 65 mm in diameter were cut from the sheets of foam produced using the semi-continuous process. Seven relative densities were tested at four different temperatures. Each temperature required 10 samples for testing to account for any variance. These foams were then tested on a Dynatup® Instrumented Impact tester and data was collected using data acquisition software on a PC following ASTM D3763-97a "Standard Test Method for High Speed Puncture Properties of Plastics Using Load and Displacement Sensors". These data points were analyzed and several points of interest were charted in data tables. A relative density for each sample set was then calculated from the foam average density and the density of the parent material. All impact tests were conducted at atmospheric pressure.

RESULTS AND DISCUSSION

Solubility Measurements

Figure 3 shows the CO_2 uptake for CPET at several saturation pressures, and the distinctive knee in the 5 MPa curve signifies crystallization as seen in previous studies[1-3]. As the sorption curve passes through the knee (maximum), the polymer begins to reject the CO_2, indicative of crystallites forming, thus decreasing the solubility. Figure 4 shows data that has been corrected for the weight percent crystallinity of CPET after various equilibrium gas concentrations are achieved. This corrected gas concentration assumes that the crystallized polymer rejects the CO_2, and so these corrected values represent the CO_2 present in the amorphous

Figure 3 CO_2 uptake for CPET saturated at several saturation pressures at 25°C

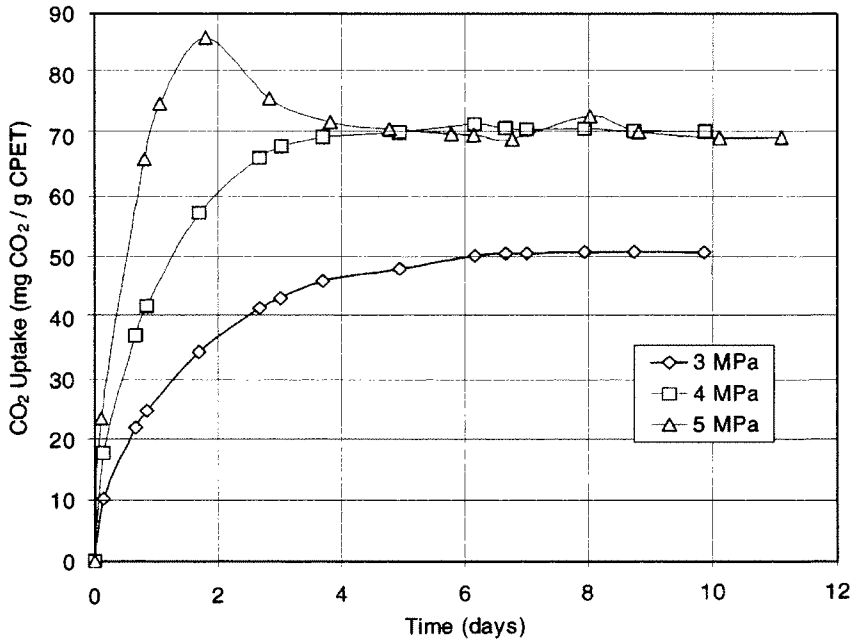

Figure 4 Equilibrium CO_2 gas concentrations corrected for weight percent crystallinity of CPET at 25°C

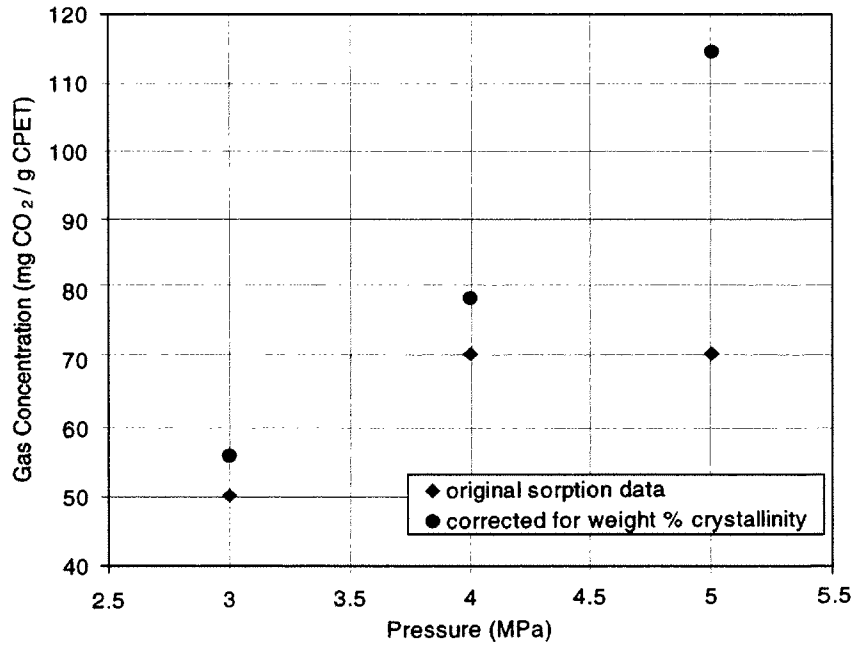

CPET. This corrected data fits the expected linear increase in equilibrium gas concentration that can be seen with increased saturation pressure seen in nearly all polymer/gas systems investigated thus far.

Foaming Experiments

The relative density, the density of the foam divided by the density of the virgin material, is plotted in Figure 5 as a function of foaming temperature for saturation pressures 3,4, and 5 MPa. Comparing data at 3 and 4 MPa, we see that with increasing saturation pressure a lower foaming temperature is needed to produce the same density foam. For the 5 MPa specimens, notice the dramatic increase in the foaming temperature needed to achieve an equal relative density compared to the 3 and 4 MPa samples. This is due to the increase in weight percent crystallinity as shown in Table 1. Table 2 gives the relative density and thickness achieved after foaming at particular conditions. Note that the saturation cycled (saturated but not foamed) specimens increased in thickness by nearly 5% over the virgin CPET.

Figure 5 Relative density versus foaming temperature for CPET saturated at several saturation pressures

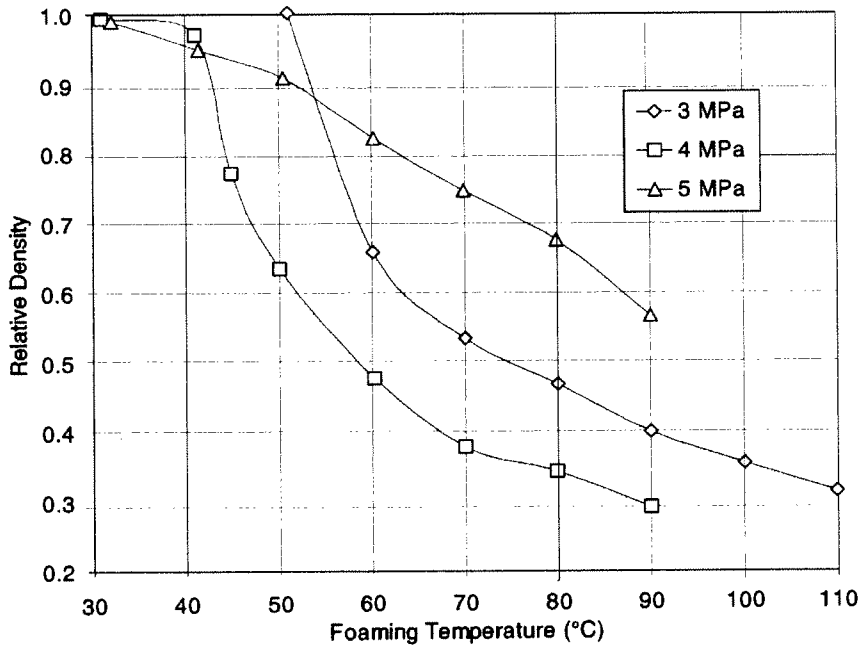

Table 1 Weight percent crystallinity for CPET saturated at various saturation pressures

Saturation pressure (MPa)	Weight % crystallinity
Virgin CPET	10.4
3	10.4
4	10.4
5	38.5

Table 2 Processing conditions and the resulting specimen density and thickness

Saturation pressure (MPa)	Foaming temperature (° C)	Relative density[1]	Specimen thickness (mm)
*	*	1.00	0.73
5	**	1.00	0.76
5	50	0.95	0.81
5	60	0.89	0.86
5	70	0.74	0.96
5	80	0.67	1.01
5	90	0.56	1.06

1. Normalized by CPET density of 1.3 g/cm^3
* Virgin CPET
** Saturation cycled CPET

Falling Weight Impact Tests (Gardner Impact)

Figure 6 shows the Gardner impact strength plotted as a function of relative density for CPET saturated at several pressures. The highest impact strength is seen in the virgin CPET at 14.1 J/mm. CPET that was saturated at 3 MPa (435 psi) and 4 MPa (580 psi) show an immediate loss of impact strength and remain fairly steady regardless of the foam relative density. CPET saturated at 5 MPa (725 psi) shows a very different behaviour, with only about a 10 percent loss in impact strength at a density reduction of nearly 40 percent. This remarkable behaviour was what lead to further investigation of impact properties using the instrumented impact equipment.

Instrumented Impact Tests

Each instrumented impact test produced a load versus time plot. The software on the Dynatup® impact tester automatically integrated the load versus deflection data, both of which vary with time during the dynamic test, to obtain energy to the point of maximum load, and the total energy to failure. The typical test lasted for approximately six milliseconds.

Figure 6 Gardner impact strength versus relative density for CPET saturated at several saturation pressures at 25°C. Twenty specimens were tested at each condition

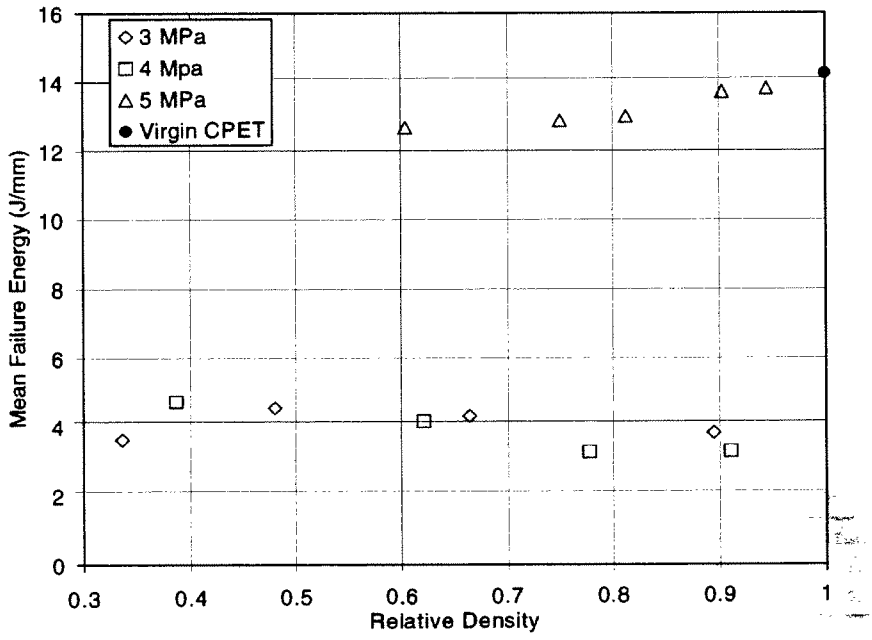

Table 3 shows the normalized failure energy data for different relative densities at different testing temperatures. The numbers for failure energy are average for ten tests. Note the first two rows show data at relative density of 1.0. The first row gives data for the as-received, unprocessed CPET specimens that we have designated as 'virgin' CPET in this paper. The second row gives impact data for 'saturation cycled' CPET specimens. These specimens were saturated with 5 MPa CO_2 and were left to desorb at room temperature for at least two months before testing. These saturation-cycled specimens provide a better approximation to the impact properties of the foam matrix material as compared to virgin CPET.

First, we note that as temperature drops, the normalized failure energy of virgin CPET drops from about 11.4 J/mm at room temperature to 5.4 J/mm at -28.9°C. Unfortunately data for virgin CPET at -40°C was not obtained, but we estimate it to be about 4 ± 1.5 J/mm for the purpose of making a general comparison. By contrast, we see that the saturation cycling clearly reduces the impact strength of CPET. This is likely due to the increase in crystallinity of the saturation cycled specimen to about 40 weight percent, compared to 10 weight percent for virgin CPET (See Table 1), rendering the saturation cycled specimens more brittle.

Table 3 Normalized failure energy in J/mm and standard deviation for instrumented impact testing of CPET at various temperatures. Ten specimens were tested at each condition

	22.2° C (72° F)		-17.8° C (0° F)		-28.9° C (-20° F)		-40.0° C (-40° F)	
Relative density	Failure energy (J.mm)	Std. Dev.	Failure energy (J/mm)	Std. Dev.	Failure energy (J/mm)	Std. Dev.	Failure energy (J/mm)	Std. Dev.
1.00*	11.37	0.15	8.12	0.60	5.40	2.13	—	—
1.00**	4.65	2.20	0.83	0.48	0.87	0.48	0.57	0.37
0.95	5.98	1.03	1.93	1.00	1.77	1.26	—	—
0.89	6.38	0.24	1.83	1.18	0.64	1.38	—	—
0.74	6.74	0.34	6.50	0.91	4.82	1.62	3.02	1.28
0.67	6.25	0.29	5.49	1.74	3.47	1.66	3.05	1.34
0.56	4.92	0.95	5.28	1.98	5.75	1.44	4.08	2.40

*Virgin CPET
**Saturation cycled CPET

The failure energy data in Table 3 has been plotted in Figure 7 as a function of the foam relative density. The earlier observation from Figure 6, namely that the Gardner impact strength is maintained by microcellular CPET to nearly virgin CPET levels up to a reduction in density of 40%, is not repeated with the room temperature tests. However, this earlier observation seems to be collaborated with the lower temperature tests. For example, the data at -28.9°C shows that failure energy initially decreases to approximately 1 J/mm for relative densities in the 0.9 to 0.95 range. However, for lower relative densities, the failure energy increases to about 5.5 J/mm, the same as for virgin CPET. This is an amazing result. To put it differently, microcellular CPET with a reduction in density of 25 to 50%, has an impact strength comparable to the virgin CPET at -28.9°C.

The room temperature data for microcellular CPET is given in the second column in Table 3. We see that the normalized failure energy for all microcellular specimens tested lies in the 4.9 to 6.7 J/mm range. Thus it appears that in the 0.55 to 0.95 relative density range the impact strength is essentially constant at about 50% of the impact strength of the virgin CPET.

The data in Tables 2 and 3 can be used to estimate the impact strength of microcellular CPET foams. First the foam thickness is estimated, and then the impact strength can be determined. To illustrate this, consider an example of a target CPET specimen with a 30% reduction in density, and let us estimate the impact strength at room temperature. At a saturation pressure of 5 MPa (725 psi), it would take a foaming temperature of approximately 74°C (166°F) to achieve this density reduction. Interpolating

the thickness data in Table 2, we estimate that this specimen would have a thickness of 0.98 mm. From Table 3, the normalized failure energy at room temperature is found to be 6.46 J/mm. After adjusting for thickness, the foam in our example will have a failure energy of 6.34 J.

Figure 8 plots normalized failure energy to maximum load as a function of the foam relative density. Data at various temperatures is included. The maximum load is simply the highest load recorded during the dynamic impact test. The trends discussed above with reference to Figure 7 can also be seen in Figure 8.

Figure 7 Failure energy for instrumented impact testing of CPET foams at various temperatures. The filled symbols give data for the unprocessed virgin CPET. The non-filled data at the relative density of 1.0 corresponds to saturation-cycled CPET

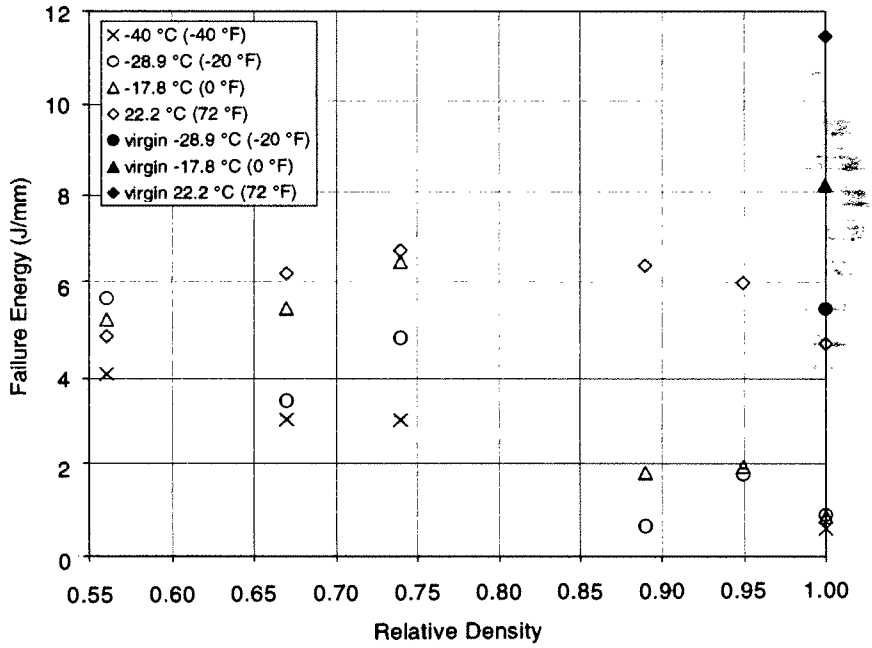

CONCLUSIONS

This study has brought out some unique properties of solid state microcellular CPET. In microcellular CPET foams obtained from fully crystallized specimens by saturating them with CO_2 at 5 MPa, it was found that up to 50% reduction in density is possible without a significant drop in impact strength. In fact, at lower temperatures, in the -17.8°C (0°F) to -40°C (-40°F) range, the impact strength of CPET foams appears to be comparable to that of the virgin polymer.

Figure 8 Energy to maximum load for instrumented impact testing of CPET at various temperatures

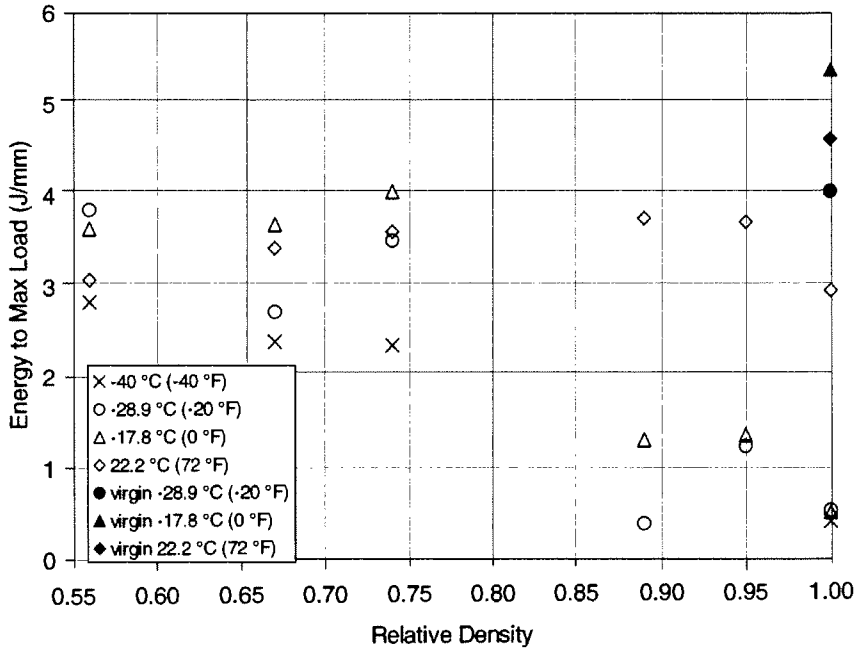

This result is very significant and has far reaching commercial implications, especially in applications where impact strength is important. Clearly, for such applications, substantial reductions in density and thus in material costs are possible without sacrificing the performance under impact loads.

ACKNOWLEDGMENTS

This research was sponsored by the UW-Industry Cellular Composites Consortium. Thanks are due to Eastman Chemical Co. for providing the materials used in this study, and to Lawson-Mardon Thermaplate Corp. for conducting the instrumented impact tests.

REFERENCES

1. Baldwin D.F. and Suh N.P., "Microcellular Poly(ethylene terephthalate) and Crystallizable Poly(ethylene terephthalate): Characterization of Process Variables", SPE Technical Papers, **38**, 1992, 1503

2. Kumar V. and Gebizlioglu O.S., "Carbon Dioxide Induced Crystallization in PET Foams", SPE Technical Papers, **37**, 1991, 1297
3. Kumar V. and Stolarczuk P.J., "Microcellular PET Foams Produced by The Solid-State Process", SPE Technical Papers, **42**, 1996, 1894
4. Mizoguchi K., Terada K., Hirose T. and Kamiya Y, "Crystallization of Poly(ethylene terephthalate) Under High-Pressure Gases", Polymer Communications, **31**, 1990, 146
5. Barlow C., Weller J., Bordia R. and Kumar V., "Solid-State Microcellular CPET Foams: The Effect of Nucleating Agents and Impact Modifiers", SPE Technical Papers, **44**, 1998, 1944
6. Kumar V., Eddy Sharon and Murray Ross, "The Solubility and Diffusivity of CO_2 in PETG", Polymer Pre-prints, American Chemical Society, **37**, No. 2, August 1996, 779
7. Kumar V. and Schirmer H.G., "Semi-Continuous Production of Solid-State PET Foams", SPE Technical Papers, **41**, 1995, 2189
8. Kumar V and Schirmer H., "Semi-Continuous Production of Solid State Polymeric Foams", US Patent #5,684,055, 1997